

1 **Human motor cortical gamma activity relates to GABAergic signalling**
2 and to behaviour

3
4 Catharina Zich^{*,1,2}, Magdalena Nowak^{*,1,2}, Emily L Hinson^{1,2}, Andrew J Quinn¹, Mark W
5 Woolrich^{1,2}, Charlotte J Stagg^{1,2,3}

6
7 * These authors contributed equally to this work.

8
9 ¹ Oxford Centre for Human Brain Activity, Wellcome Centre for Integrative Neuroimaging,
10 Department of Psychiatry, University of Oxford

11 ² Wellcome Centre for Integrative Neuroimaging, FMRIB, Nuffield Department of Clinical
12 Neurosciences, University of Oxford

13 ³ Medical Research Council Brain Network Dynamics Unit, University of Oxford, UK

14
15
16 Corresponding author:
17 Catharina Zich

18 catharina.zich@uni-oldenburg.de
19 Wellcome Centre for Integrative Neuroimaging, FMRIB
20 Nuffield Department of Clinical Neurosciences
21 University of Oxford

22
23 **Keywords**
24 GABA, MEG, Motor learning, Motor system, TMS

1 Key Points

- 2 We combined neuroimaging (i.e. MEG) and non-invasive brain stimulation (i.e. TMS)
3 to examine the properties of γ activity sub-bands in the primary motor cortex.
- 4 Two distinct γ sub-bands (slow- γ , mid- γ) show a movement-related increase in
5 activity during finger movements and are characterised by distinct temporal-spectral-
6 spatial profiles.
- 7 We found strong evidence for a positive relationship between slow- γ (~30-60Hz)
8 peak frequency and endogenous GABA signalling during movement preparation (as
9 assessed using the TMS-metric short interval intracortical inhibition).

10 Abstract

11 Gamma activity (γ , >30 Hz) is universally demonstrated across brain regions and species.
12 However, the physiological basis and functional role of γ sub-bands (slow- γ , mid- γ , fast- γ) have
13 been predominantly studied in rodent hippocampus; γ activity in the human neocortex is
14 much less well understood.

15 Here we combined neuroimaging and non-invasive brain stimulation to examine the
16 properties of γ activity sub-bands in the primary motor cortex (M1), and their relationship to
17 both local GABAergic activity and to motor learning. In 33 healthy individuals, we quantified
18 movement-related γ activity in M1 using magnetoencephalography, assessed GABAergic
19 signaling using transcranial magnetic stimulation (TMS), and estimated motor learning via a
20 serial reaction time task.

21 We characterised two distinct γ sub-bands (slow- γ , mid- γ) which show movement-related
22 increase in activity during unilateral index finger movements and are characterised by distinct
23 temporal-spectral-spatial profiles. Bayesian correlation analysis revealed strong evidence for
24 a positive relationship between slow- γ (~30-60Hz) peak frequency and endogenous GABA
25 signalling during movement preparation (as assessed using the TMS-metric short interval
26 intracortical inhibition). There was also moderate evidence for a relationship between power
27 of the movement-related mid- γ activity (60-90Hz) and motor learning. These relationships
28 were neurochemically- and frequency-specific.

29 These data provide new insights into the neurophysiological basis and functional roles of γ
30 activity in human M1 and allow the development of a new theoretical framework for γ activity
31 in the human neocortex.

1 **Significance Statement**

2 Gamma (γ) activity is ubiquitous in the brain, yet our understanding of the mechanisms and
3 function of γ activity in the human neocortex, and particularly in the human motor cortex, is
4 limited. Using a multimodal approach, we characterised two patterns of movement-related γ
5 activity in the human motor cortex (slow- γ and mid- γ), with different spatial, temporal and
6 spectral properties. Slow- γ peak frequency was correlated to local GABA-A activity, whereas
7 mid-gamma power predicted performance in a subsequent motor learning task. Based on
8 these findings and previous research, we propose a theoretical framework to explain how
9 human motor cortical γ activities may arise and their potential role in plasticity and motor
10 learning, providing new hypotheses to be tested in future studies.

1 1 Introduction

2
3 Activity within the gamma band (γ , >30 Hz) is ubiquitous across the mammalian brain. This
4 broad frequency band is commonly divided into three sub-bands: slow- γ (human: ~30-60Hz;
5 rodent: ~30-50Hz), mid- γ (human: ~60-90Hz; rodent: ~50-100 Hz) and fast- γ (human: >90 Hz;
6 rodent: >100 Hz). To date, γ activity has been mainly explored in rodent hippocampus, where
7 the sub-bands of this activity arise from separate locations (Schomburg et al., 2014; Lasztóczki
8 and Klausberger, 2016), reflect distinct microcircuits (Bragin et al., 1995; Colgin et al., 2009;
9 Fernández-Ruiz et al., 2017), and have different functional roles (Carr and Frank, 2012; Colgin,
10 2015). Considerably less is known about the neurophysiological bases and functional roles of
11 the γ sub-bands in the human neocortex.

12
13 In the human motor system, a movement-related increase in γ power (γ event-related
14 synchronization [γ ERS]) has been described (Crone et al., 1998; Pfurtscheller and Lopes da
15 Silva, 1999; Canolty et al., 2006; Cheyne et al., 2008; Muthukumaraswamy, 2010, 2011;
16 Cheyne, 2013). This has been most frequently reported for the mid- γ band (i.e. mid- γ ERS),
17 which occurs only during actual rather than imagined movement (Muthukumaraswamy,
18 2011), shows spatial specificity to the primary motor cortex (M1, (Crone et al., 2006)) and
19 temporal specificity to the time of the movement. Mid- γ has been suggested to play a role in
20 afferent proprioceptive feedback or relate to more active motor control processes (Miller et
21 al., 2010; Muthukumaraswamy, 2010), and its pro-kinetic role has been demonstrated in a
22 number of studies (Joundi et al., 2012; Swann et al., 2016, 2018). In humans, slow- γ has been
23 considerably less well characterised. Only few studies have reported movement-related slow- γ
24 activity in the M1 (Crone et al., 1998; Szurhaj et al., 2006). Their data suggested that slow- γ
25 has a distinct spatio-temporal profile and plays a functional role in synchronising activity of
26 neuronal populations involved in movement.

27
28 Slow- γ and mid- γ likely share some physiological similarities. Empirical animal studies and
29 computational modelling have demonstrated that GABAergic interneuron-mediated
30 inhibition of pyramidal cell activity generates γ activity in M1 (Gonzalez-Burgos and Lewis,
31 2008; Sohal et al., 2009; Buzsáki and Wang, 2012). Despite initial findings in humans relating
32 γ activity in M1 to GABA (Gaetz et al., 2011) it remains to be determined how closely these
33 data, which arise from in vitro and invasive in vivo recordings, translate into the γ ERS seen in

1 human electrophysiological recordings. However, given the wealth of data implicating
2 changes in M1 GABAergic activity during motor learning (Stagg et al., 2011), γ activity may
3 reflect a mechanism by which decreases in local GABAergic signalling mediates behavioural
4 improvements. In line with this hypothesis, our group recently demonstrated that 75 Hz tACS
5 applied to M1 leads to a significant reduction in local GABA-A activity, as assessed by
6 transcranial magnetic stimulation (TMS, (Nowak et al., 2017)). Moreover, this 75 Hz tACS-
7 induced change in GABA-A activity was closely correlated with an individual's motor learning
8 ability.

9

10 The present study aims to investigate the relationship between M1 GABAergic signalling, M1
11 γ activity and motor learning in humans. We characterized M1 γ activity in 33 young healthy
12 individuals during unilateral index finger movement using magnetoencephalography (MEG),
13 to address the hypotheses that an individual's M1 movement-related γ activity is related to
14 TMS measure of local GABA-A activity and the ability to learn a motor task.

1 **2 Methods**

2 **2.1 Participants**

3 33 individuals (age 24.9 years, range: 21–30 years; 14 male) gave their informed consent to
4 participate in the study in accordance with Central University Research Ethics Committee
5 approval (University of Oxford; MSD-IDREC-C2–2014-026 and MSD-IDREC-C1-2015-010). All
6 participants were right-handed as assessed by the Edinburgh Handedness Inventory (Oldfield,
7 1971), had no history of neurological or psychiatric disorders, no metal implants, and reported
8 no other contraindications to TMS or MEG. A subset of these data formed part of a previous
9 publication (Nowak et al., 2017).

10 **2.2 Experimental Design**

11 All individuals completed all parts of the study on the same day in the following order: MEG
12 data recording during rest and during a Go/NoGo task, a motor learning task (ML) and a
13 response time task (RT) outside the MEG, and TMS during rest and RT task (**Fig. 1a**).

14 **MEG data acquisition**

15 MEG data were acquired with a whole-head 306-channel Elektro Neuromag system (204 planar
16 gradiometers, 102 magnetometers). Concurrent surface electromyography (EMG) of the right
17 extensor digitorum communis and first dorsal interosseous (FDI) muscle were recorded using
18 bipolar surface electrodes. Both MEG and EMG data were sampled at 1000 Hz with a band-
19 pass filter of 0.03-330 Hz. Head position was continuously monitored with respect to the MEG
20 sensors using four head-position (HPI) coils. The locations of HPI coils and of three anatomical
21 fiducials (the nasion and two preauricular points) were digitized using a 3D tracking system
22 (Polhemus, EastTrach 3D) to define the subject-specific cartesian head coordinate system. In
23 addition, vertical and horizontal electrooculogram electrodes were used to allow for detection
24 and removal of eye-blink artefacts. MEG data were acquired during a Go/NoGo task. A blue
25 circle cue, presented for 200 ms, instructed participants to prepare for an abduction of the
26 index finger of their right hand. The cue was then replaced by a fixation cross for 1000 ms (cue
27 - stimulus interval). A subsequent visual stimulus presented for 200 ms (coloured circle: green
28 for Go or red for NoGo) indicated whether they should perform (Go) or withhold (NoGo) the
29 prepared response. Participants were instructed to respond as quickly as possible on the Go
30 trials. The stimulus was then replaced by a fixation cross for a duration that varied randomly
31 trials. The stimulus was then replaced by a fixation cross for a duration that varied randomly
32 trials.

1 between 2000 and 4000 ms (inter-trial interval). The task consisted of a total of 70 trials and
2 lasted ~5 min. NoGo trials (20% of all trials) were introduced to encourage participants'
3 attention to the task. Stimuli were generated using the MATLAB Psychophysics Toolbox
4 version 3.0 package (Brainard, 1997) and back-projected (Panasonic DLP Projector, PT
5 D7700E) onto a screen at a viewing distance of 120 cm with a spatial resolution of 1024 by
6 768 pixels and a refresh rate of 60 Hz.

7

8 Motor learning task

9 Outside the MEG, individuals performed a visually cued motor sequence learning task which
10 has been described previously (Nowak et al., 2017). Briefly, individuals were presented with
11 four horizontal bars on a screen, each of which corresponded to a key on the keyboard. When
12 a bar changed into an asterisk, individuals were instructed to press the corresponding key as
13 quickly and accurately as possible. The task included sequence blocks consisting of three
14 repeats of a 10-item sequence. The first and 15th blocks consisted of 30 visual cues presented
15 in a random order.

16

17 Response time task

18 Individuals performed also a simple RT task consisting of 20 trials to characterize their
19 individual RT for the subsequent TMS measurement. Individuals were instructed to respond
20 to a visual Go signal (coloured green circle) by performing an index finger abduction of the
21 right hand as quickly as possible. Visual stimuli appeared at random intervals (5-7 s) and the
22 individuals were instructed to avoid anticipation of the Go signal and to relax their hand while
23 the fixation cross was displayed on the screen. Stimuli were generated using the MATLAB
24 Psychophysics Toolbox version 3.0 package (Brainard, 1997). Surface EMG was recorded via
25 disposable neonatal ECG electrodes (Henley's Medical) from the FDI of the right hand using a
26 belly-tendon montage with a ground electrode over the ulnar styloid process. Signals were
27 sampled at 5 kHz, amplified, filtered (10-1000 Hz), and recorded using a CED 1902 amplifier, a
28 CED micro1401 A/D converter, and Signal software version 3.13 (Cambridge Electronic
29 Design).

30

1 TMS data acquisition

2 All TMS data were acquired using a monophasic BiStim machine connected to a 70 mm figure-
3 of-eight coil (Magstim). The left M1 FDI motor hotspot, i.e. the position where single-pulse
4 motor evoked potentials (spMEPs) could be elicited in the right FDI muscle at the lowest
5 stimulator intensity, was targeted. The TMS coil was held at 45° to the midsagittal line with
6 the handle pointing posteriorly. The hotspot was marked on a tight-fitting cap to ensure
7 reproducible coil positioning. Surface EMG data were recorded in the same manner as during
8 the RT task.

9

10 First, resting motor threshold (rMT) and active motor threshold (aMT) were determined. rMT
11 was defined as the minimum stimulus intensity required for eliciting spMEPs of ~1 mV peak-
12 to-peak amplitude in at least 5/10 trials in the relaxed FDI muscle. aMT was defined as the
13 minimum stimulus intensity necessary to evoke spMEPs of ~200 µV peak-to-peak amplitude
14 in at least 5/10 trials while individuals maintained ~30% of the maximum contraction of the
15 FDI.

16

17 Local GABA-A synaptic activity was assessed using short interval intracortical inhibition (SICI)
18 with an interstimulus interval of 2.5 ms (Kujirai et al., 1993; Di Lazzaro et al., 2005). The
19 conditioning stimulus was set at 70% of aMT and the test stimulus at rMT. spMEP and SICI
20 were measured in pseudorandomized order with fifteen trials per condition, both at rest and
21 during the pre-movement period of the simple RT task (same RT task as performed prior to
22 TMS). TMS measures were collected at two different times during movement preparation: an
23 early time point (25% of mean RT) and a late time point (65% of mean RT), resulting in four
24 different pre-movement protocols: spMEP_{early}, spMEP_{late}, SICI_{early} and SICI_{late}. The 25% and 65%
25 RT were adjusted to each individual's mean RT according to a previously described procedure
26 (Murase et al., 2004; Hummel et al., 2009). Fifteen trials per condition and time point were
27 recorded.

28

29 2.3 Data analysis

30 MEG data analysis

31 External noise was reduced from MEG data by means of spatio-temporal signal-space
32 separation (TSSS) and head movements (detected using HPI coils) corrected, both using

1 MaxMove software as implemented in MaxFilter version 2.1 (Elektas Neromag, Elektas,
2 Stockholm, Sweden). Further MEG data analyses were performed using the in-house OHBA
3 Software Library (OSL: <https://ohba-analysis.github.io/osl-docs/>) version 2.2.0. Registration
4 between a structural MRI template, i.e. MNI152 standard-space T1-weighted average
5 structural template image, and MEG data was performed with RHINO (Registration of
6 Headshapes Including Nose in OSL) using nose and fiducial landmarks for coregistration and a
7 single shell as forward model.

8

9 Continuous data were down-sampled to 500 Hz. Further, a band-pass filter (5-245 Hz) and
10 several notch filters were applied (49-55 Hz, 99-101 Hz, 149-151 Hz, 199-201 Hz). A wider
11 notch filter around 50 Hz was used to suppress 50 Hz line noise and a 53 Hz artefact present in
12 this dataset caused by the HPI coils. Time segments containing artefacts were identified by
13 using generalized extreme studentized deviate method (GESD (Rosner, 1983)) at a significance
14 level of 0.05 with a maximum number of outliers limited to 20% of the data on the standard
15 deviation of the signal across all sensors in 1 s non-overlapping windows. The windows
16 corresponding to outliers were excluded from all further analysis. Further denoising was
17 applied using independent component analysis (ICA) using temporal FastICA across sensors
18 (Hyvärinen, 1999). 62 independent components were estimated and components
19 representing stereotypical artefacts such as eye blinks, eye movements, and electrical
20 heartbeat activity were manually identified and regressed out of the data. Data then were
21 filtered into three frequency bands (β 13-30 Hz, slow- γ 30-60 Hz, mid- γ 60-90 Hz) and the
22 following processing steps were performed separately for the three frequency bands.

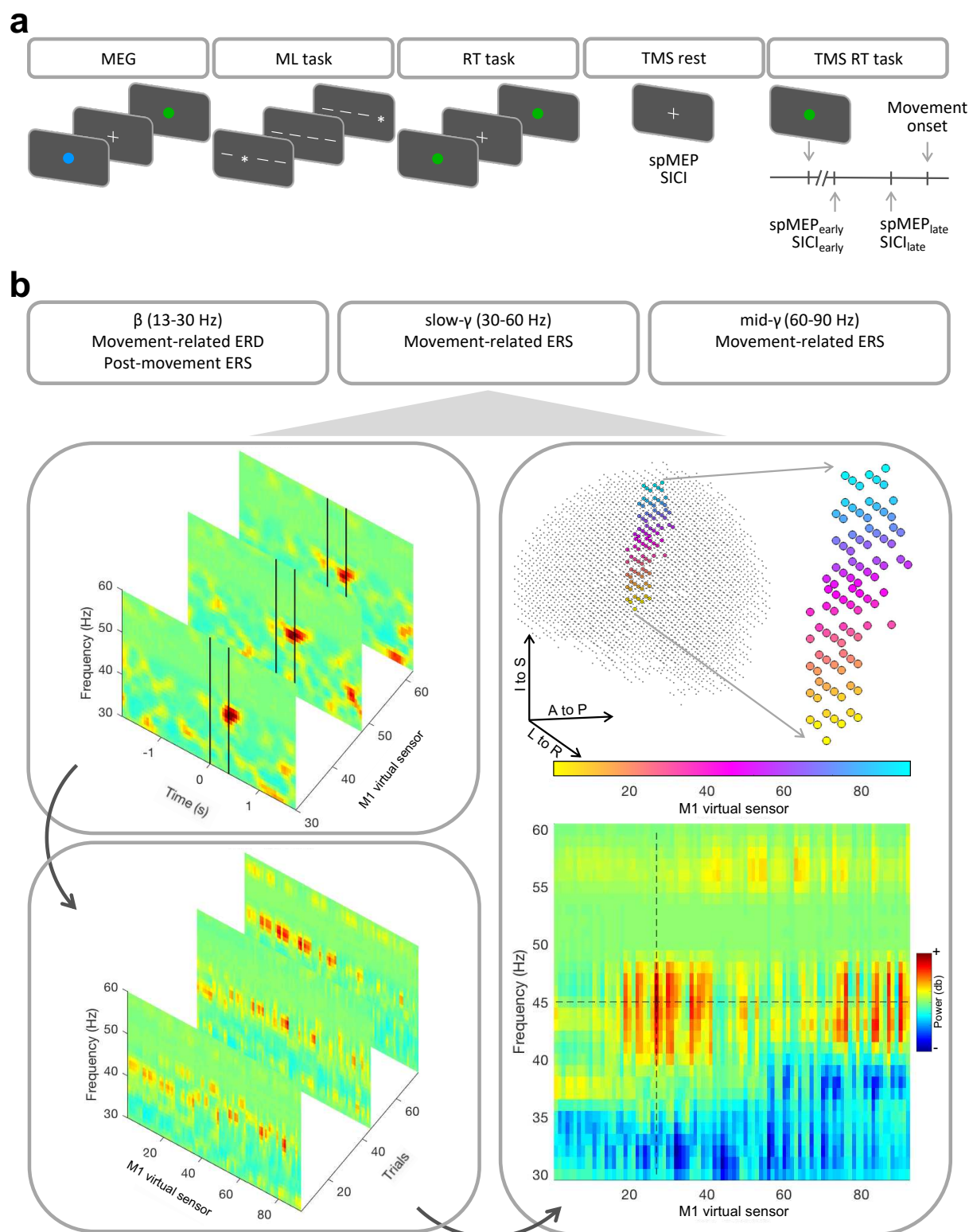
23

24 Magnetometers and Planar-Gradiometers were normalized by computing the eigenvalue
25 decomposition across sensors within each coil type and dividing the data by the smallest
26 eigenvalue within each (Woolrich et al., 2011). Data were projected onto an 8 mm grid in
27 source space (resulting in 3559 virtual sensors) using a Linearly Constrained Minimum
28 Variance (LCMV) vector beamformer (Van Veen and Buckley, 1988; Woolrich et al., 2011).
29 Beamformer weights were estimated across an 8 mm grid cast within the inner-skull of the
30 MNI152 brain. A covariance matrix was computed across the whole time-course and was
31 regularized to 50 dimensions using principal component analysis (PCA) rank reduction (Quinn
32 et al., 2018).

1 Epochs were defined relative to the movement onset (movement offset for β ERS) as
2 identified by surface EMG. To identify movement onset and offset EMG data were first high-
3 pass filtered at 10 Hz. EMG data were then segmented from -1 s to 3 s relative to the Go
4 stimuli, and the envelope (root mean square, window = 80 ms), computed. Using a non-
5 overlapping moving standard deviation (movement onset: window = 24 ms, direction =
6 forward; movement offset: window = 120 ms, direction = backwards) movement onset and
7 offset were defined as the first window exceeding the threshold (three standard deviations of
8 the EMG activity between -600 ms to -200 ms relative to Go stimuli). Trials were excluded
9 when the envelope, the reaction time (i.e. time between Go stimuli and movement onset), or
10 the movement time (i.e. time between movement onset and offset) were identified as outliers
11 using GESD at a significance level of 0.05. This approach results in 45.59 (SD = 4.88) out of 56
12 epochs per individual. MEG data were segmented from -2 s to 2 s relative to movement onset
13 (movement offset for β ERD).

15
16 Time-frequency analysis was applied to single trials and virtual sensors using dpss-based
17 multitaper (window = 1.6 s, steps = 200 ms) with a frequency resolution of 1 Hz. Segments
18 were baseline corrected (-1 s to -0.5 s, [-1.5 s to -1 s for β ERD]) using the mean baseline across
19 all trials. This procedure results in trial-by-trial time-frequency decomposition for each of the
20 3559 virtual sensors. To detect the individual peak frequency within each frequency band only
21 the virtual sensors within M1, following the Desikan-Killiany atlas, (N = 92) were considered.
22 Trial-wise movement-related power was obtained by averaging across time, i.e. from
23 movement onset to movement offset (from movement offset to movement offset + 1 s for β
24 ERS) and then averaged across trials. The maximum (minimum for β ERD) of the resulting two-
25 dimensional matrix containing the power between movement on- and offset across trials at
26 each frequency within the frequency band at each virtual sensor was defined as an individual's
27 power and defined the individual's peak frequency and virtual sensor (**Fig. 1b**).

28
29 To illustrate the spatial properties of movement-related responses we computed the
30 movement-related power (as above, first averaging across time, i.e. from movement onset to
31 movement offset [from movement offset to movement offset + 1 s for β ERS] and then
32 averaged across trials) at the individual's peak frequency for each of the 3559 virtual sensors.



1
2 **Fig.1** (a) Experimental timeline. MEG data were recorded while individuals performed a
3 Go/NoGo task (70 trials). Each trial started with a preparation cue (blue circle, for 200 ms),
4 followed by a cue-stimulus interval (fixation cross, 1000 ms) and the Go (green circle, 80% of
5 the trials) or NoGo (red circle) cue. After the MEG participants performed a visually cued
6 motor sequence learning (ML) task (4 fingers, 10-item sequence, 3 repeats per block, 15
7 blocks). Individuals also performed a simple response time (RT) task (20 trials) to determine
8 their individual RT. Each trial started with a green circle indicating to perform an index finger
9 abduction followed by a fixation cross indicating the inter-trial interval. TMS measures (single-

1 pulse MEP [spMEP] and short interval intracortical inhibition [SICI]) were performed at rest
2 and during the RT task. During the RT task, spMEP and SICI were obtained at two different
3 timings during movement preparation: an early time point (25% of mean RT, spMEP_{early},
4 SICI_{early}) and a late time point (65% of mean RT, spMEP_{late}, SICI_{late}). (b) Pipeline used to identify
5 the individuals' peak frequency for β ERD, β ERS, slow- γ ERS, mid- γ ERS, exemplary for one
6 individual for slow- γ ERS. For each individual trial the power from movement onset to
7 movement offset (movement offset to movement offset + 1 s for β ERS), as determined by
8 EMG and indicated by the black vertical lines, was averaged for each frequency band and
9 virtual sensors within the M1 separately (top left). This resulted in movement-related power
10 (post-movement-related power for β ERS) for each frequency, M1 virtual sensor and trial
11 (bottom left). The maximum (minimum for β ERD) of the average across trials (right) indicates
12 the individuals' power, peak frequency (dashed horizontal line) and virtual sensor within M1
13 (dashed vertical line). Virtual sensors are ordered based on MNI z-coordinates and color-
14 coded accordingly (e.g. small index = yellow = inferior).

15

16 Motor learning data analysis

17 To derive an accurate motor learning score, individual RTs (i.e. time from cue onset to the
18 correct button press) were first evaluated. Anticipatory responses (i.e. those that occurred
19 before the cue) and outliers (i.e. RTs outside of the mean value ± 2 SD per each block) were
20 discarded. A motor learning score was calculated for each individual as a percentage change
21 from the RT in the first sequence block (block 2) to blocks 10-14, when the learning plateaued
22 (Stagg et al., 2011). Thus, more negative motor learning scores represent better performance.
23 One individual was excluded from this analysis due to noncompliance with instructions.

24

25 Response time task data analysis

26 EMG data were analysed online using Signal software version 3.13 (Cambridge Electronic
27 Design). RT was identified for each trial as the time interval between the Go signal and the
28 onset of EMG activity recorded above the FDI muscle (i.e. mV first data point where EMG
29 amplitude >0.1 mV). The mean RT was then used in the remainder of that experimental
30 session to calculate the timing of the pre-movement TMS pulses.

31

32 MEP data analysis

33 Trials were excluded if the test pulse alone failed to elicit a reliable MEP (amplitude <0.1 mV),
34 there was precontraction in the target FDI muscle (EMG amplitude >0.1 mV in the 80 ms
35 preceding the pulse), or, for the pre-movement TMS measures, EMG onset coincided with
36 TMS pulse or no response was made. The peak-to-peak amplitude for each MEP was then
37 calculated. Any MEPs outside of the mean value ± 2 SD for each condition for each block were

1 excluded. Next, a single iteration of Grubbs' test with a significance level of 0.05 was
2 performed for each TMS condition separately and any significant outliers excluded.
3 Collectively, these rejection criteria resulted in the exclusion of <5 trials per individual in any
4 condition. SICI and ICF were expressed as a ratio of the mean conditioned MEP amplitude to
5 the mean unconditioned MEP amplitude. For the pre-movement data, the TMS measures
6 were analysed separately for each pre-movement time point (25% and 65% RT).

7

8 2.4 Statistical analysis

9 All Frequentist statistics were conducted as implemented in SPSS version 25 (SPSS Inc,
10 Chicago, IL, USA). As Bayesian inference allows multiple hypotheses to be tested and can
11 calculate the probability that one hypothesis is true relative to another hypothesis, correlation
12 analysis was performed using Bayesian inference (JASP, JASP Team 2019, version 0.11.1) with
13 default priors after outlier removal. The Bayes factors (BFs) is the ratio of the likelihood of one
14 particular hypothesis to the likelihood of another. We categorise BFs based using the heuristic
15 classification scheme for BF_{10} (Lee and Wagenmakers, 2013, p.105; adjusted from Jeffreys,
16 1961). Thus, for example, $BF_{10} = 10-30$ denotes strong evidence, $BF_{10} = 3-10$ moderate, and
17 $BF_{10} = 1-3$ anecdotal evidence for H_1 , while $BF_{10} = 1/3-1$ denotes anecdotal, $BF_{10} = 1/10-1/3$
18 moderate, and $BF_{10} = 1/30-1/10$ strong evidence for H_0 . Outliers were identified for each
19 correlation separately by bootstrapping the Mahalanobis distance (Schwarzkopf et al., 2012).
20 To statistically compare correlations, Fisher's z-transformation was applied to each correlation
21 coefficient, resulting in normally distributed values r' with standard errors $s_{r'}$. The null
22 hypotheses ($r'_1 - r'_2 = 0$) were tested in R(psych) (Revelle, 2015) using Student t test (Howell,
23 2011). Reported p -values are 2-tailed.

1 **3 Results**

2 **3.1 MEG reveals expected ERD and ERS in the beta band**

3 Clear movement-related changes in power were observed in all three frequency bands (β ,
4 slow- γ , mid- γ), characterized by different spectra-temporal-spatial properties. We observed a
5 clear β ERD during movement and a β ERS after movement termination. In line with previous
6 studies, the β ERD started before movement onset, plateaued between movement onset and
7 offset, and terminated after movement offset (**Fig. 2a**, bottom left). The mean β ERD peak
8 frequency was 19.33 Hz (range 15-26 Hz). There was moderate evidence for a lack of
9 relationship between peak frequency and power ($r = 0.011$, $BF_{10} = 0.22$) across individuals.
10 Again, consistent with prior observations, the β ERS started after movement offset and lasted
11 for roughly 1 s (**Fig. 2a**, bottom right). The mean β ERS peak was 18.21 Hz (range 14-25 Hz).
12 There was anecdotal evidence for a lack of relationship between peak frequency and power
13 ($r = -0.284$, $BF_{10} = 0.74$).

14

15 **3.2 Two distinct patterns of movement-related γ activity**

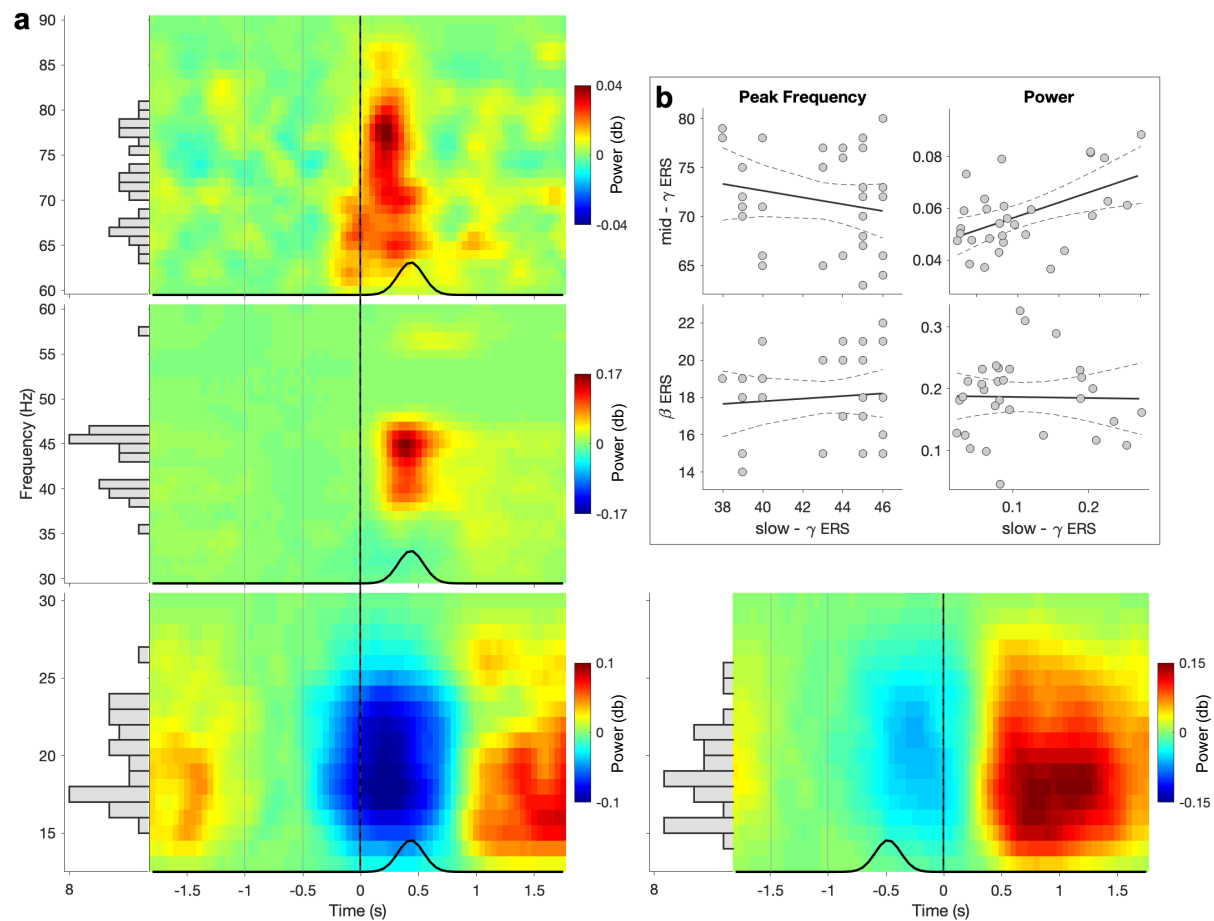
16 We then wanted to investigate movement-related activity in the γ bands. In the slow- γ band
17 we observed a strong ERS, which started after movement onset, reached its peak at the time
18 of movement offset, and decreased after movement offset, suggesting that the slow- γ ERS
19 was temporally aligned with movement offset (**Fig. 2a**, center left). The mean slow- γ peak
20 frequency was 43.06 Hz (range 35-57 Hz), and moderate evidence for a lack of relationship
21 between peak frequency and power was found ($r = -0.034$, $BF_{10} = 0.22$). In the mid- γ band we
22 also observed an ERS. This ERS started at movement onset, reached its peak between
23 movement onset and offset, and terminated around movement offset (**Fig. 2a**, top left),
24 therefore showing a temporal alignment with movement, unlike the slow- γ ERS. The mean
25 mid- γ peak frequency was at 71.36 Hz (range 63-80 Hz), and there was anecdotal evidence for
26 a lack of relationship between peak frequency and power ($r = 0.249$, $BF_{10} = 0.55$).

27

28 To our knowledge, while movement-related slow- γ has been reported previously (Crone et al.,
29 1998; Szurhaj et al., 2006), its properties have not been fully characterised. We therefore
30 sought to investigate whether this pattern of neural activity was distinct from the movement-
31 related β ERS and mid- γ ERS. We performed four Bayesian pairwise correlations to test
32 whether the peak frequency or power of the slow- γ ERS was related to these measures

1 derived from the β ERS or mid- γ ERS (Fig. 2b). We found moderate evidence for a lack of
2 relationship between slow- γ ERS and β ERS peak frequency ($r = -0.196$, $BF_{10} = 0.38$) and
3 anecdotal evidence for a lack of relationship between slow- γ ERS and mid- γ ERS peak
4 frequency ($r = 0.088$, $BF_{10} = 0.26$). In terms of power, there was moderate evidence for a lack
5 of a relationship between slow- γ ERS and β ERS ($r = -0.019$, $BF_{10} = 0.22$), but strong evidence
6 for a relationship between slow- γ ERS and mid- γ ERS ($r = 0.514$, $BF_{10} = 12.61$).

7

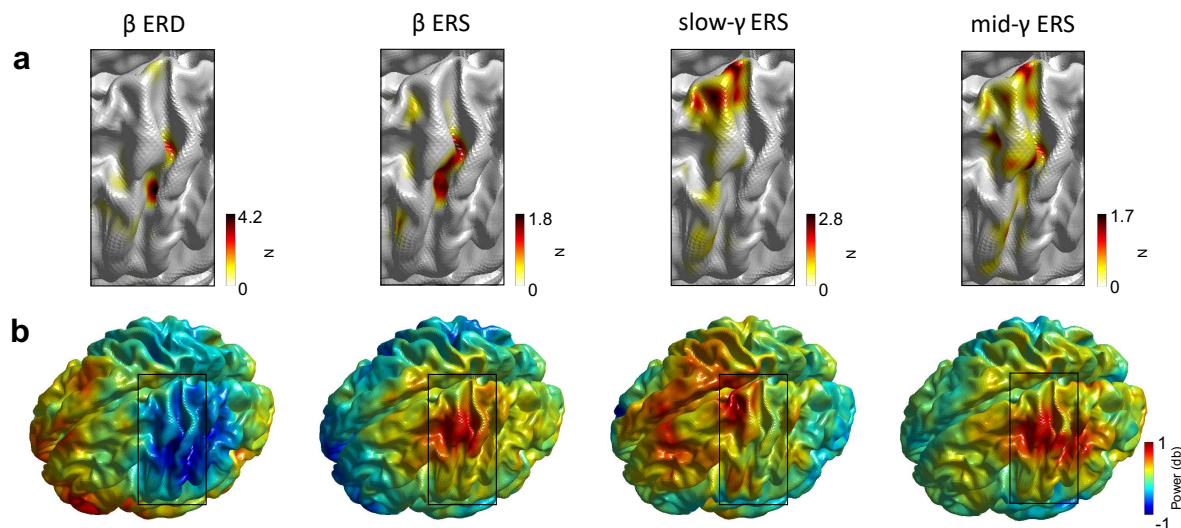


8
9 **Fig.2** Temporal and spectral properties of movement-related responses. (a) Changes in power
10 relative to baseline (-1 to -0.5 s relative to movement onset [-1.5 to -1 s relative to movement
11 offset for β ERS], as indicated by the grey vertical lines). Data are locked to movement onset
12 (movement offset for β ERS, as identified by EMG and highlighted by the black vertical line).
13 Black line represents the distribution of movement offsets (movement onsets for β ERS) of
14 trials included in the analysis. Side panel histograms illustrate the distribution of individual
15 peak frequency (bin size = 1 Hz). (b) Correlations for peak frequency (left) and power (right)
16 between slow- γ ERS and β ERS (bottom) as well as slow- γ ERS and mid- γ ERS (top). Dashed
17 lines represent the 95% confidence intervals.
18

19 Next, we examined the spatial properties of the movement-related slow- γ ERS compared with
20 the β ERD, β ERS and mid- γ ERS. We considered the group-heatmaps of the peak virtual

1 sensors and power maps. In line with previous findings, the group-heatmaps of the peak
2 virtual sensors for β ERD and β ERS were relatively focal with the hotspot posterior and
3 relatively central on the superior-inferior axis within the M1 (**Fig. 3a**). In contrast, the hotspot
4 for the slow- γ was more superior and central on the anterior-posterior axis. Finally, the
5 heatmap for the mid- γ was less focal, encompassing the hotspot of the β and the slow- γ
6 frequency range.

7
8 The spatial pattern of the power maps was qualitatively comparable for β ERD, β ERS and mid-
9 γ with peaks in central on the superior-inferior axis and the anterior-posterior axis within M1
10 (**Fig. 3b**). In contrast, the spatial map of the slow- γ was qualitatively more anterior within the
11 M1 and extended to frontal areas.



12
13 **Fig.3** Spatial properties of movement-related responses. (a) Heatmap of the number of
14 selected virtual sensors within M1. For visualisation data are interpolated. (b) Power maps,
15 i.e. power averaged from movement onset to movement offset (movement offset to
16 movement offset + 1 s) at each of the 3559 virtual sensors at the individuals' peak
17 frequency (i.e. frequency with strongest positive [negative for β ERD] power change from
18 baseline within M1).

19
20 3.3 Slow- γ ERS peak frequency is related to individuals' GABA-A activity during
21 movement preparation

22 Next, we investigated the neurophysiological underpinnings of the movement-related activity
23 we observed. In line with our hypothesis that movement-related activity in the γ band is
24 related to movement-related GABA-A activity, we found strong evidence for a positive
25 relationship between pre-movement SICI amplitude and slow- γ peak frequency ($r = 0.677$,
26 $BF_{10} = 18.13$). There was moderate evidence for a lack of relationship between pre-movement

1 SICI amplitude and peak frequency in other bands (β ERD: $r = -0.010$, $BF_{10} = 0.29$; β ERS: $r =$
2 0.061 , $BF_{10} = 0.29$; mid- γ : $r = 0.07$, $BF_{10} = 0.295$, **Fig. 4**, left). The observed relationship between
3 pre-movement SICI and slow- γ peak frequency was significantly different from the
4 relationships observed in other bands (SICI and slow- γ peak frequency vs SICI and β ERD peak
5 frequency: $z = -2.26$, $p = 0.024$; SICI and slow- γ peak frequency vs SICI and β ERS peak
6 frequency: $z = -2.10$, $p = 0.036$; SICI and slow- γ peak frequency vs SICI and mid- γ peak
7 frequency: $z = -2.07$, $p = 0.039$).

8

9 Having demonstrated a significant relationship between pre-movement SICI and slow- γ peak
10 frequency, we then wished to explore the temporal specificity of this effect. Therefore, we
11 investigated the relationship between pre-movement SICI and slow- γ peak frequency, for
12 SICI_{early} and SICI_{late} separately, in post-hoc analyses. There was anecdotal evidence for a
13 positive relationship between slow- γ peak frequency and GABA-A activity early in movement
14 preparation (SICI_{early}, $r = 0.433$, $BF_{10} = 1.78$) and strong evidence for a positive relationship
15 between slow- γ peak frequency and GABA-A activity late in movement preparation (SICI_{late}, r
16 = 0.641 , $BF_{10} = 10.41$). There was no significant different between these two correlations ($z =$
17 -0.84 , $p = 0.401$). There were no significant correlations between the peak frequency of any
18 band and subsequent motor learning.

19

20 3.4 Mid- γ power correlates with subsequent motor learning

21 Finally, we wished to investigate the behavioural importance of these movement-related
22 signals.

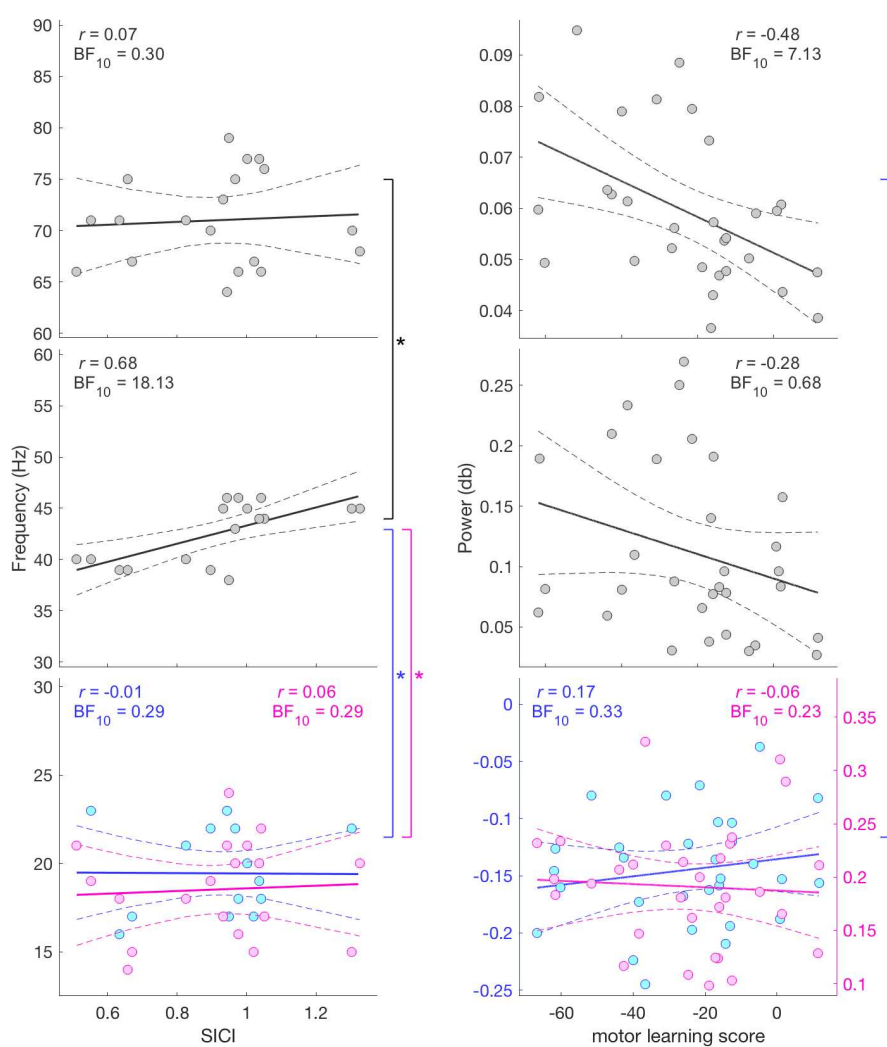
23

24 Firstly, it was important to determine whether participants were able to learn the task. As
25 expected, RT decreased significantly across successive sequence blocks ($F_{(14,336)} = 9.015$; $p <$
26 0.001). In contrast, there was no significant difference in mean RT between the two random
27 blocks ($t_{(32)} = 0.885$; $p = 0.383$), whereas there was a significant difference between block 14
28 (the final learning block) and block 15 (the second random block) ($t_{(28)} = -6.899$; $p < 0.001$),
29 suggesting that improvements in RT occurred via learning of a specific sequence and not
30 generic skill learning. There was also no significant difference between the RT from blocks 10-
31 14, which were on the plateau of the learning curve ($F_{(4,108)} = 0.440$; $p = 0.780$).

32

1 In line with our hypothesis, we found moderate evidence for a negative relationship between
2 motor learning score and mid- γ power ($r = -0.481$, $BF_{10} = 7.13$, **Fig. 4** right), such that higher
3 mid- γ power was related to greater motor learning. There was moderate evidence for a lack
4 of relationship between motor learning score and power in other bands (β ERD: $r = 0.166$, BF_{10}
5 = 0.33; β ERS: $r = -0.056$, $BF_{10} = 0.23$; slow- γ : $r = -0.281$, $BF_{10} = 0.684$). The observed relationship
6 between motor learning score and mid- γ power was different from the relationship between
7 motor learning score and β ERD power ($z = -2.55$, $p = 0.011$) and β ERS power ($z = -1.72$, $p =$
8 0.085). There were no significant relationships between the power in any band and SICI.

9



10

11 **Fig.4** Relationship between MEG peak frequency and SICI amplitude (left) and MEG power and
12 motor learning score (right) for β ERD (bottom blue), β ERS (bottom pink), slow- γ (middle) and
13 mid- γ (top). Dashed lines represent the 95% confidence intervals. $^{\circ} p < 0.1$, $* p < 0.5$.

14

1 **4 Discussion**

2 This work aimed to examine the physiological basis and functional significance of movement-
3 related M1 γ activity. We identified two distinct patterns of movement-related γ activity in
4 M1, characterised by different temporal-spectral-spatial properties. We went on to
5 investigate the physiological correlates of these, and identified a correlation between M1
6 slow- γ peak frequency and pre-movement SICI amplitude in M1, such that individuals with a
7 higher slow- γ peak frequency showed less GABA-A activity. Finally, in line with previous work
8 we found that a higher M1 mid- γ power was related to better individual performance in a
9 motor learning task.

10

11 **4.1 Two distinct movement-related patterns of γ activity**

12 Animal studies and human direct cortical recordings have suggested the presence of two
13 distinct patterns of activity within the γ band in M1, but until now it has proved difficult to
14 robustly separate them with transcranial approaches. By optimising our MEG analysis, i.e.
15 separate beamformer for each sub-band and high-precision peak frequency/spatial location
16 estimation, we have demonstrated the presence of two movement-related γ activity patterns
17 within M1.

18

19 Given the paucity of previous transcranial studies focussing on slow- γ movement-related
20 activity, we first examined whether the slow- γ activity seen here represented a distinct neural
21 activity pattern, or was merely an extension of either post-movement β ERS or movement
22 mid- γ ERS. We then reasoned that if the slow- γ ERS reflected activity within the same local
23 microcircuits as either the post-movement β ERS or movement mid- γ ERS we would expect to
24 observe systematic relationships on a subject-by-subject basis between slow- γ and β or mid- γ . We only found a relationship between slow- γ ERS power and mid- γ ERS power. The absence
25 of other relationships add weight to the hypothesis that the slow- γ ERS is a distinct movement-
26 related activity pattern but is in itself not conclusive. We therefore went on to investigate both
27 the temporal and spatial domain of the slow- γ ERS, demonstrating that it is dissociable from
28 both the post-movement β ERS and movement mid- γ ERS in both of these domains. Slow- γ
29 ERS appeared to be temporally aligned with the movement offset, rather than movement
30 onset, like the mid- γ ERS, or post-movement, like β ERS, and has a spatial distribution that is
31 more frontal than either the mid- γ ERS, which is more localised to M1 or the beta-ERS.
32

1
2 Taken together, the data suggest that two distinct patterns of movement-related γ activity are
3 seen in the human M1. The next question we aimed to address is the likely cellular basis of
4 these two distinct γ activity patterns.
5

6 4.2 Slow- γ activity likely arises from superficial cortical layers

7 A commonly held hypothesis states that activity in the lower cortical layers is predominantly
8 slower than that in the more superficial layers (i.e. frequency-layer gradient), reflecting the
9 different functional roles of superficial and deep layers. This is supported by animal studies in
10 primary sensory areas (e.g. (Roopun et al., 2006; Buffalo et al., 2011; Spaak et al., 2012;
11 Haegens et al., 2015)). Moreover, human laminar MEG showed that visual α activity and
12 sensorimotor β activity localise more to the white matter surface approximating infragranular
13 origin than to the pial surface, while visual and sensorimotor γ activity localise more to the
14 pial surface approximating supragranular origin than to the white matter surface (Bonaiuto et
15 al., 2018). However, there is also evidence challenging the frequency-layer gradient by
16 suggesting deeper cortical layers as origin for γ activity. For example, in the visual cortex of
17 behaving mice, γ activity has been linked to parvalbumin (PV)-positive GABAergic
18 interneurons (Chen et al., 2017), which are most densely populated in layer V (Fagiolini et al.,
19 2004; Sohal et al., 2009). Further, auditory *in vitro* work revealed two distinct γ activities, 30-
20 45 and 50-80 Hz, originating in layer II/III and layer IV, respectively (Ainsworth et al., 2011).
21 The precise neural basis of γ activity in the primary M1, as opposed to primary sensory regions,
22 has yet to be determined (Whittington et al., 2011). Translating the findings directly from
23 studies performed in the sensory areas to M1 must be done with care, as the circuit
24 organisation of M1 differs fundamentally from that of sensory areas, not least in that it is
25 agranular, lacking a distinct layer IV (Shipp, 2005; Shipp et al., 2013).
26

27 To explore whether M1 movement-related β and/or γ activity arises from superficial cortical
28 layers, we tested the relationship between β , slow- γ and mid- γ and SICI amplitude, a direct
29 measure of local cortical GABA-A activity, quantified via TMS. TMS preferentially stimulates
30 more superficial neurons, particularly at the intensities used here (Siebner et al., 2009).
31 Further, computational modelling studies have demonstrated that TMS effects can be
32 explained by activity within the canonical microcircuit, which includes layer II/III and layer V

1 excitatory pyramidal cells, inhibitory interneurons, and cortico-cortical and thalamo-cortical
2 inputs (Di Lazzaro and Ziemann, 2013). We demonstrated a specific relationship between local
3 GABA-A activity and slow- γ activity, which was not observed for either the β or mid- γ activity.
4 Importantly, different microcircuits within M1 have distinct patterns of GABA-A receptor
5 morphology in terms of their α subunits. SICI has been demonstrated to primarily represent
6 activity within cortical microcircuits involving interneurons that express GABA-A receptors
7 with α -2 and α -3 subunits, rather than α -1 (Di Lazzaro et al., 2007). α -1 subunits are found at
8 highest density in layer V of the healthy human M1, whereas α -2 subunits are more common
9 in the superficial layers, and α -3 are fairly equally distributed across the cortical layers (Freund,
10 2003; Petri et al., 2003).

11
12 In summary, the data presented here suggest that movement-related slow- γ activity arises
13 from neuronal circuits containing layer II/III interneurons. The functional role of movement-
14 related slow- γ activity is less clear. Previous work has postulated that it may directly reflect
15 motor output (Crone et al., 1998).

16
17 4.3 Mid- γ activity may reflect activity in learning-related microcircuits
18 In light of the significant correlation between slow- γ and SICI amplitude the absence of the
19 same relationship for mid- γ could be interpreted in at least two ways. First, in human M1 slow-
20 γ and mid- γ stem both from superficial layers, but from different populations or
21 microcircuits, with the one underlying slow- γ , but not mid- γ , being GABAergic as measured
22 using SICI. This would be in line with the frequency-layer gradient reported in sensory areas
23 (Roopun et al., 2006; Buffalo et al., 2011; Spaak et al., 2012; Haegens et al., 2015; Bonaiuto et
24 al., 2018).

25
26 Second, while slow- γ arises superficially mid- γ arises from deeper layers, such as layer V. This
27 is in conformity with other animal work in sensory areas (Sohal et al., 2009; Ainsworth et al.,
28 2011; Chen et al., 2017) and the supported by the functional role of M1 mid- γ . We
29 demonstrated that the power of mid- γ activity elicited by a simple movement predicted the
30 ability to learn a motor skill on a subject-by-subject basis. This is in line with previous work.
31 For example, we have shown that an individual's response to 75 Hz tACS relates to their ability
32 to learn a subsequent motor skill (Nowak et al., 2017), and further, when amplitude

1 modulated by an underlying theta pattern, improves motor learning in healthy adults (Akkad
2 et al., 2019). The finding of a specific relationship between mid- γ activity and plasticity is
3 consistent with data from animal recordings suggesting that microcircuits containing α -1
4 GABA-A synapses, predominantly found in the PV-rich layer V in M1, are a major neural
5 substrate for plasticity, at least in the visual cortex (Fagiolini et al., 2004). Together, the origin
6 of mid- γ activity is not completely understood, but mid- γ activity seems to play a role in motor
7 learning.

8

9 4.4 Limitations

10 This study used non-invasive recordings to indirectly study changes in movement-related
11 activity in the motor cortex. While this approach provides an unrivalled ability to understand
12 activity in the healthy human system, it has inherent limitations in terms of the conclusions
13 we can draw. Specifically, here, it was difficult to accurately quantify activity around 50 Hz due
14 to power line noise. In addition, due to an artefact caused by the HPI coils at 53 and 54 Hz, we
15 had to widen the standardly-employed line noise notch filter to 49-55 Hz. This had direct
16 implications on our assessment of the peak frequency of slow- γ ERS.

17

18 4.5 Conclusions

19 The findings presented here allow us to create a theoretical framework for γ activity in the
20 human M1, as follows: there are two patterns of movement-related γ activity in the human
21 motor cortex (slow- γ and mid- γ), with differential temporal, spectral and spatial properties.
22 The frequency of movement-related slow- γ activity is related to our neurophysiological
23 measure of GABA-A activity, but does not play a direct role in motor plasticity *in vivo*. We
24 conclude that slow- γ arises from alpha-2 and alpha-3 GABA-A microcircuits in layer II/III. Mid- γ
25 activity predicts motor learning, but whether it originates layer II/III or V is not yet clear. This
26 framework draws together findings from this paper and the literature, and provides a number
27 of hypotheses that can be directly tested.

1 **Acknowledgements**

2 We thank Miles Whittington for helpful discussions on the functional role of gamma activity.

3

4 **Funding**

5 CJS holds a Sir Henry Dale Fellowship, funded by the Wellcome Trust and the Royal Society
6 (102584/Z/13/Z). MN is funded by the Wellcome Trust. MWW's research is supported by the
7 Wellcome Trust (106183/Z/14/Z, 215573/Z/19/Z), and by the New Therapeutics in
8 Alzheimer's Diseases (NTAD) study supported by UK MRC and the Dementia Platform UK. The
9 laboratory space and equipment were supported by the University of Oxford John Fell Fund
10 and the Wellcome Trust Institutional Strategic Support Fund (to CJS). The work was supported
11 by the NIHR Oxford Health Biomedical Research Centre and the NIHR Biomedical Research
12 Centre Oxford. The Wellcome Centre for Integrative Neuroimaging is supported by core
13 funding from the Wellcome Trust (203139/Z/16/Z).

14

15 **Data availability**

16 Data are available from the first authors and the last author upon request.

17

18 **Competing Interests**

19 No conflict of interest is declared.

20

21 **Author contributions**

22 MN and CJS designed the study. MN, EH and CZ collected the data. CZ and MN analysed the
23 data. AJQ and MWW provided assistance with data analysis. CJS supervised the project. CZ,
24 MN and CJS wrote the manuscript and EH, AJQ and MWW edited the manuscript.

25

26 **References**

27 Ainsworth M, Lee S, Cunningham MO, Roopun AK, Traub RD, Kopell NJ, Whittington MA
28 (2011) Dual gamma rhythm generators control interlaminar synchrony in auditory
29 cortex. *J Neurosci* 31:17040–17051.

30 Akkad H, Dupont-Hadwen J, Frese A, Tetkovic I, Barrett L, Bestmann S, Stagg CJ (2019)
31 Increasing motor skill acquisition by driving theta-gamma coupling.

1 bioRxiv:2019.12.20.883926 Available at:
2 <http://biorxiv.org/content/early/2019/12/20/2019.12.20.883926.abstract>.

3 Bonaiuto JJ, Meyer SS, Little S, Rossiter H, Callaghan MF, Dick F, Barnes GR, Bestmann S
4 (2018) Lamina-specific cortical dynamics in human visual and sensorimotor cortices.
5 *Elife* 7:1–32.

6 Bragin A, Jando G, Nadasdy Z, Hetke J, Wise K, Buzsaki G (1995) Gamma (40-100 Hz)
7 oscillation in the hippocampus of the behaving rat. *J Neurosci* 15:47–60.

8 Brainard D (1997) The Psychophysics Toolbox. *Spat Vis* 10:433–436.

9 Buffalo EA, Fries P, Landman R, Buschman TJ, Desimone R (2011) Laminar differences in
10 gamma and alpha coherence in the ventral stream. *Proc Natl Acad Sci U S A* 108:11262–
11 11267.

12 Buzsáki G, Wang X-J (2012) Mechanisms of gamma oscillations. *Annu Rev Neurosci* 35:203–
13 225.

14 Canolty RT, Edwards E, Dalal SS, Soltani M, Nagarajan SS, Kirsch HE, Berger MS, Barbaro NM,
15 Knight RT (2006) High gamma power is phase-locked to theta oscillations in human
16 neocortex. *Science* (80-) 313:1626–1628.

17 Carr MF, Frank LM (2012) A single microcircuit with multiple functions: State dependent
18 information processing in the hippocampus. *Curr Opin Neurobiol* 22:704–708 Available
19 at: <http://dx.doi.org/10.1016/j.conb.2012.03.007>.

20 Chen G, Zhang Y, Li X, Zhao X, Ye Q, Lin Y, Tao HW, Rasch MJ, Zhang X (2017) Distinct
21 Inhibitory Circuits Orchestrate Cortical beta and gamma Band Oscillations. *Neuron*
22 96:1403-1418.e6 Available at: <https://doi.org/10.1016/j.neuron.2017.11.033>.

23 Cheyne D (2013) MEG studies of sensorimotor rhythms: a review. *Exp Neurol* 245:27–39.

24 Cheyne D, Bells S, Ferrari P, Gaetz W, Bostan AC (2008) Self-paced movements induce high-
25 frequency gamma oscillations in primary motor cortex. *Neuroimage* 42:332–342
26 Available at: <http://www.ncbi.nlm.nih.gov/pubmed/18511304> [Accessed February 14,
27 2018].

28 Colgin LL (2015) Do slow and fast gamma rhythms correspond to distinct functional states in
29 the hippocampal network? *Brain Res* 1621:309–315 Available at:
30 <http://dx.doi.org/10.1016/j.brainres.2015.01.005>.

31 Colgin LL, Denninger T, Fyhn M, Hafting T, Bonnevie T, Jensen O, Moser MB, Moser EI (2009)
32 Frequency of gamma oscillations routes flow of information in the hippocampus.

- 1 Nature 462:353–357.
- 2 Crone N, Sinai A, Korzeniewska A (2006) High-frequency gamma oscillations and human
- 3 brain mapping with electrocorticography. *Prog Brain Res* 159:275–295.
- 4 Crone NE, Miglioretti DL, Gordon B, Lesser RP (1998) Functional mapping of human
- 5 sensorimotor cortex with electrocorticographic spectral analysis. II. Event-related
- 6 synchronization in the gamma band. *Brain* 121 (Pt 1):2301–2315 Available at:
- 7 <http://www.ncbi.nlm.nih.gov/pubmed/9874481> [Accessed February 14, 2018].
- 8 Di Lazzaro V, Oliviero A, Saturno E, Dileone M, Pilato F, Nardone R, Ranieri F, Musumeci G,
- 9 Fiorilla T, Tonali P (2005) Effects of lorazepam on short latency afferent inhibition and
- 10 short latency intracortical inhibition in humans. *J Physiol* 564:661–668.
- 11 Di Lazzaro V, Pilato F, Dileone M, Profice P, Ranieri F, Ricci V, Bria P, Tonali PA, Ziemann U
- 12 (2007) Segregating two inhibitory circuits in human motor cortex at the level of GABA_A
- 13 receptor subtypes: A TMS study. *Clin Neurophysiol* 118:2207–2214.
- 14 Fagiolini M, Fritschy JM, Löw K, Möhler H, Rudolph U, Hensch TK (2004) Specific GABA_A
- 15 Circuits for Visual Cortical Plasticity. *Science* (80-) 303:1681–1683.
- 16 Fernández-Ruiz A, Oliva A, Nagy GA, Maurer AP, Berényi A, Buzsáki G (2017) Entorhinal-CA3
- 17 Dual-Input Control of Spike Timing in the Hippocampus by Theta-Gamma Coupling.
- 18 *Neuron* 93:1213–1226.e5.
- 19 Freund TF (2003) Interneuron Diversity series: Rhythm and mood in perisomatic inhibition.
- 20 *Trends Neurosci* 26:489–495.
- 21 Gaetz W, Edgar JC, Wang DJ, Roberts TPL (2011) Relating MEG measured motor cortical
- 22 oscillations to resting γ -aminobutyric acid (GABA) concentration. *Neuroimage* 55:616–
- 23 621 Available at: <https://pubmed.ncbi.nlm.nih.gov/21215806>.
- 24 Gonzalez-Burgos G, Lewis DA (2008) GABA neurons and the mechanisms of network
- 25 oscillations: implications for understanding cortical dysfunction in schizophrenia.
- 26 *Schizophr Bull* 34:944–961.
- 27 Haegens S, Barczak A, Musacchia G, Lipton ML, Mehta AD, Lakatos P, Schroeder CE (2015)
- 28 Laminar profile and physiology of the α rhythm in primary visual, auditory, and
- 29 somatosensory regions of neocortex. *J Neurosci* 35:14341–14352.
- 30 Howell D (2011) Statistical methods for psychology. Wadsworth: Cengage Learning.
- 31 Hummel FC, Steven B, Hoppe J, Heise K, Thomalla G, Cohen LG, Gerloff C (2009) Deficient
- 32 intracortical inhibition (SICI): During movement preparation after chronic stroke.

- 1 Neurology 72:1766–1772.
- 2 Hyvarinen A (1999) Fast and robust fixed-point algorithms for independent component
- 3 analysis. IEEE Trans Neural Networks 10:626–634 Available at:
- 4 <http://ieeexplore.ieee.org/document/761722/> [Accessed May 11, 2018].
- 5 Joundi RA, Jenkinson N, Brittain JS, Aziz TZ, Brown P (2012) Driving oscillatory activity in the
- 6 human cortex enhances motor performance. Curr Biol 22:403–407 Available at:
- 7 <http://dx.doi.org/10.1016/j.cub.2012.01.024>.
- 8 Kujirai T, Caramia M, Rothwell J, Day B, Thompson P, Ferbert A, Wroe S, Asselman P,
- 9 Marsden C (1993) Corticocortical inhibition in human motor cortex. J Physiol (1993),
- 10 471:501–519.
- 11 Lasztóczki B, Klausberger T (2016) Hippocampal Place Cells Couple to Three Different Gamma
- 12 Oscillations during Place Field Traversal. Neuron 91:34–40.
- 13 Miller KJ, Schalk G, Fetz EE, den Nijs M, Ojemann JG, Rao RPN (2010) Cortical activity during
- 14 motor execution, motor imagery, and imagery-based online feedback. Proc Natl Acad
- 15 Sci U S A 107:4430–4435.
- 16 Murase N, Duque J, Mazzocchio R, Cohen LG (2004) Influence of somatosensory input on
- 17 motor function in patients with chronic stroke. Ann Neurol 55:400–409.
- 18 Muthukumaraswamy SD (2010) Functional Properties of Human Primary Motor Cortex
- 19 Gamma Oscillations. J Neurophysiol 104:2873–2885 Available at:
- 20 <http://www.ncbi.nlm.nih.gov/pubmed/20884762> [Accessed February 14, 2018].
- 21 Muthukumaraswamy SD (2011) Temporal dynamics of primary motor cortex gamma
- 22 oscillation amplitude and piper corticomuscular coherence changes during motor
- 23 control. Exp Brain Res 212:623–633.
- 24 Nowak M, Hinson E, van Ede F, Pogosyan A, Guerra A, Quinn A, Brown P, Stagg CJ (2017)
- 25 Driving Human Motor Cortical Oscillations Leads to Behaviorally Relevant Changes in
- 26 Local GABA_A Inhibition: A tACS-TMS Study. J Neurosci 37:4481–4492 Available at:
- 27 <http://www.jneurosci.org/lookup/doi/10.1523/JNEUROSCI.0098-17.2017>.
- 28 Petri S, Krampfl K, Hashemi F, Grothe C, Hori A, Dengler R, Bufler J (2003) Distribution of
- 29 GABA_A receptor mRNA in the motor cortex of ALS patients. J Neuropathol Exp Neurol
- 30 62:1041–1051.
- 31 Pfurtscheller G, Lopes da Silva FH (1999) Event-related EEG/MEG synchronization and
- 32 desynchronization: basic principles. Clin Neurophysiol 110:1842–1857.

- 1 Quinn AJ, Vidaurre D, Abeysuriya R, Becker R, Nobre AC, Woolrich MW (2018) Task-Evoked
- 2 Dynamic Network Analysis through Hidden Markov Modelling. *Front Neurosci*.
- 3 Revelle W (2015) *psych: Procedures for Personality and Psychological Research*.
- 4 Roopun AK, Middleton SJ, Cunningham MO, LeBeau FEH, Bibbig A, Whittington MA, Traub
- 5 RD (2006) A beta2-frequency (20-30 Hz) oscillation in nonsynaptic networks of
- 6 somatosensory cortex. *Proc Natl Acad Sci U S A* 103:15646–15650.
- 7 Rosner B (1983) Percentage Points for a Generalized ESD Many-Outlier Procedure.
- 8 *Technometrics* 25:165 Available at:
- 9 <https://www.jstor.org/stable/1268549?origin=crossref> [Accessed May 11, 2018].
- 10 Schomburg EW, Fernández-Ruiz A, Mizuseki K, Berényi A, Anastassiou CA, Koch C, Buzsáki G
- 11 (2014) Theta Phase Segregation of Input-Specific Gamma Patterns in Entorhinal-
- 12 Hippocampal Networks. *Neuron* 84:470–485.
- 13 Schwarzkopf DS, De Haas B, Rees G (2012) Better Ways to Improve Standards in Brain-
- 14 Behavior Correlation Analysis. *Front Hum Neurosci* 6:1–6.
- 15 Shipp S (2005) The importance of being agranular: a comparative account of visual and
- 16 motor cortex. *Philos Trans R Soc London Ser B, Biol Sci* 360:797–814.
- 17 Shipp S, Adams RA, Friston KJ (2013) Reflections on agranular architecture: predictive coding
- 18 in the motor cortex. *Trends Neurosci* 36:706–716.
- 19 Siebner HR, Hartwigsen G, Kassuba T, Rothwell JC (2009) How does transcranial magnetic
- 20 stimulation modify neuronal activity in the brain? Implications for studies of cognition.
- 21 *Cortex* 45:1035–1042 Available at: <http://dx.doi.org/10.1016/j.cortex.2009.02.007>.
- 22 Sohal VS, Zhang F, Yizhar O, Deisseroth K (2009) Parvalbumin neurons and gamma rhythms
- 23 enhance cortical circuit performance. *Nature* 459:698–702 Available at:
- 24 <http://dx.doi.org/10.1038/nature07991>.
- 25 Spaak E, Bonnefond M, Maier A, Leopold DA, Jensen O (2012) Layer-specific entrainment of
- 26 gamma-band neural activity by the alpha rhythm in monkey visual cortex. *Curr Biol*
- 27 22:2313–2318 Available at: <http://dx.doi.org/10.1016/j.cub.2012.10.020>.
- 28 Stagg CJ, Bachtiar V, Johansen-Berg H (2011) The role of GABA in human motor learning.
- 29 *Curr Biol* 21:480–484 Available at: <http://dx.doi.org/10.1016/j.cub.2011.01.069>.
- 30 Swann NC, de Hemptinne C, Miocinovic S, Qasim S, Wang SS, Ziman N, Ostrem JL, San
- 31 Luciano M, Galifianakis NB, Starr PA (2016) Gamma Oscillations in the Hyperkinetic
- 32 State Detected with Chronic Human Brain Recordings in Parkinson's Disease. *J Neurosci*

- 1 36:6445–6458 Available at:
- 2 <http://www.jneurosci.org/lookup/doi/10.1523/JNEUROSCI.1128-16.2016>.
- 3 Swann NC, De Hemptinne C, Thompson MC, Miocinovic S, Miller AM, Gilron R, Ostrem JL,
- 4 Chizeck HJ, Starr PA (2018) Adaptive deep brain stimulation for Parkinson's disease
- 5 using motor cortex sensing. *J Neural Eng* 15.
- 6 Szurhaj W, Labyt E, Bourriez J-L, Kahane P, Chauvel P, Mauguière F, Derambure P (2006)
- 7 Relationship between intracerebral gamma oscillations and slow potentials in the
- 8 human sensorimotor cortex. *Eur J Neurosci* 24:947–954 Available at:
- 9 <http://www.ncbi.nlm.nih.gov/pubmed/16930422> [Accessed February 14, 2018].
- 10 Van Veen BD, Buckley KM (1988) Beamforming: A Versatile Approach to Spatial Filtering.
- 11 *IEEE ASSP Mag* 5:4–24.
- 12 Whittington MA, Cunningham MO, LeBeau FEN, Racca C, Traub RD (2011) Multiple origins of
- 13 the cortical gamma rhythm. *Dev Neurobiol* 71:92–106.
- 14 Woolrich M, Hunt L, Groves A, Barnes G (2011) MEG Beamforming using Bayesian PCA for
- 15 Adaptive Data Covariance Matrix Regularisation. *Neuroimage* 57:1466–1479.
- 16